Journal of Asian Earth Sciences 251 (2023) 105674

Contents lists available at ScienceDirect

Journal of Asian Earth Sciences

journal homepage: www.elsevier.com/locate/jseaes

Processes controlling the Mg isotope behavior during granite weathering

BaiLing Fan [a,b,1], XiangQin Yang [a,1], Ke Jiang [a], ZhiQi Zhao [c,*]

[a] College of Eco-Environmental Engineering, Guizhou Minzu University, Guiyang 550025, China
[b] State Key Laboratory of Environmental Geochemistry, Institute of Geochemistry, Chinese Academy of Sciences, Guiyang 550081, China
[c] School of Earth Science and Resources, Chang'an University, Xi'an 710054, China

ARTICLE INFO

Keywords:
Granite weathering
Pedogenic carbonates
Clay minerals
Mg isotope

ABSTRACT

Silicate weathering is a fundamental process for global materials cycling and the climate regulation. Magnesium (Mg) isotope ratios have been widely used as a natural tracer to study weathering processes and biogeochemical cycles in critical zone. The geochemical behavior of Mg isotopes, however, remains unclear during granite weathering. Here, 23 saprolite samples and two bedrocks in one granite profile from Longnan county, Jiangxi province have been analyzed for their Mg isotopic composition, major elemental and REE concentration, to understand Mg isotope behavior and its controlling factors during granite weathering. In general, bulk regolith is enriched in heavier Mg isotope (-0.37‰~0.27‰) compared to the parental granite (-0.42‰) with one exception (-0.53‰). Saprolites have much lower MgO contents ranging from 28% to 49% (normalized to Ti) relative to parental rock. These show that weathering of granite is accompanied by Mg loss and formation of secondary Mg-bearing clay minerals, which preferentially adsorb heavy Mg isotope. This is reinforced by the positive relationship between δ^{26}Mg values and the content of kaolinite and gibbsite during the early weathering stage. Particularly, the soils most enriched in heavy Mg isotope are also characterized by the highest content of gibbsite. While Fe oxides is shown to make a significant influence over the soil δ^{26}Mg as weathering proceed by adsorbing light Mg isotope. More importantly, our study provides the first evidence that the impact of pedogenic carbonates is significant by shifting δ^{26}Mg towards lighter values in granite saprolite, based on the covariation of geochemical parameters, such as the CaO content, LOI and REE_S. This implies that if secondary carbonates are widespread in silicate soils, the contribution of silicate weathering to dissolved Mg fluxes may have been overestimated. And it may be an important C reservoir in terrestrial, which significantly influences the global C cycle.

1. Introduction

Chemical weathering of silicates plays an important role in regulating global climate change on tectonic timescales. During this process, atmospheric CO_2 is consumed through the neutralisation of carbonic acid and precipitation of calcium (Ca) and magnesium (Mg) bearing carbonates over geological time-scales (Berner et al., 1983; Gaillardet et al., 1999; Liu et al., 2023). In parallel, chemical weathering has a great influence on the global cycling of materials and the nutrient supply to ecosystems. In turn, such process controls the river composition, and then influence chemical composition of seawater (Gaillardet et al., 1999; Jiang et al., 2018; Liu et al.,2018).

As a major component in both soil and rivers, Mg is directly involved in the rock weathering. In the weathering processes, Mg is partitioned into hydrosphere, biosphere and pedosphere, which is also accompanied by fractionation of Mg isotopes, resulted in about 8‰ range of Mg isotopic variation for terrestrial samples in the critical zone (Schmitt et al., 2012; Teng et al., 2010, Teng, 2017; Tipper et al., 2010; Huang et al., 2012; Opfergelt et al., 2014; Lara et al., 2017). It was generally thought that ^{26}Mg was preferential incorporated into secondary clay minerals formed during rock weathering, thus driving the residual regolith to be isotopically heavier (Teng et al., 2010; Tipper et al., 2010; Huang et al., 2012; Opfergelt et al., 2014; Lara et al., 2017). While this is not always in certain, saprolites at some horizons in weathering profiles were observed to be enriched in light Mg isotopes (Huang et al., 2012; Ma et al., 2015) compared to parental silicate bedrock. Experimental studies also suggested that clay minerals formation can preferentially incorporate both light and heavy Mg isotope (Wimpenny et al., 2010; Ryu et al.,

* Corresponding author.
E-mail address: zhaozhiqi@chd.edu.cn (Z. Zhao).
[1] These authors contributed to the work equally and should be regarded as co-first authors.

https://doi.org/10.1016/j.jseaes.2023.105674
Received 14 December 2022; Received in revised form 27 March 2023; Accepted 10 April 2023
Available online 11 April 2023

2016; Hindshaw et al., 2020). However, the formation of pedogenic carbonates has always been shown to enrich in light Mg isotope, potentially driving bulk soil δ^{26}Mg to lower values (Trostle, 2013; Wimpenny et al., 2014; Oskierski et al., 2019). Overall, the direction of Mg isotope fractionation is highly dependent on primary and secondary phase mineralogy, weathering intensity and the proportions of isotopically distinct Mg species, and field conditions (Wimpenny et al., 2010, 2013; Huang et al., 2012; Liu et al., 2014; Opfergelt et al., 2014; Ryu et al., 2016; Oskierski et al., 2019; Hindshaw et al., 2020). Apart from chemical weathering, the presence of vegetation also can modify the Mg isotopic composition of the soils by preferentially absorbing heavy Mg isotope and recycling of isotopically light Mg plant material (Black et al., 2008; Bolou-Bi et al., 2012; Ryu et al., 2020). Thus far, the mechanisms controlling Mg retention in the soil and the secondary phases driving the isotope fractionation have not been well understood. The fractionation direction and magnitude are still highly in debate both in field investigations and experimental studies. Consequently, understanding the details of the controls on Mg isotope variations during weathering will be key to developing them a powerful tracer for studying physico-chemical processes.

Weathering profiles offer an unparalleled opportunity to study continental weathering processes and geochemical cycle of elements in a critical zone because its continuity in time. To date, the majority of studies focus on basalt weathering, as which is thought to play a key role in the carbon cycle, with representing up to 30% of atmospheric CO_2 consumption by the weathering of continental rocks (Huang et al., 2012; Liu et al., 2014; Ryu et al., 2020). In comparison, limited Mg isotopic data is available for weathering of granite, although it constitutes ~ 25% of the land surface of the upper crust (Oliva et al., 2003). Moreover, there is a big difference between basalt and granite, such as the mineral constitute, weathering rate and so on. For example, the abundant Mg bearing minerals in the basalt, primarily pyroxene, are more readily weathered than biotite in the granite (Brewer et al., 2018). As a major parental phyllosilicate, chlorite also plays an important role in the Mg isotope geochemistry for granite weathering profile, while secondary clay minerals, such as kaolin minerals, illite, gibbsite, are predominant for basalt weathering profile (Huang et al., 2012; Brewer et al., 2018; Ryu et al., 2020; Li et al., 2021). In addition, the experimental studies suggest that the dissolution of granite is different from that observed in basalt. Differential dissolution of minerals controlled the variation in dissolved δ^{26}Mg values for granite weathering, while Mg isotope fractionation during secondary mineral formation had a much greater influence on basalt weathering (Wimpenny et al., 2010; Ryu et al., 2011). As yet, only two granitic zones have been investigated and there is little information on the distribution of Mg isotopes amongst weathering residues. One granite weathering profile suggested that illite predominantly controlled the saprolites, while the other was related to the evolving of chlorite (Brewer et al., 2018; Li et al., 2021). These phenomena reflect that the Mg isotope geochemistry is enigmatic.

To improve our knowledge on the behavior of Mg isotope during chemical weathering, here, a weathering profile developed on granite in a subtropical monsoon climate in Longnan county, Jiangxi province in southeast of China is chosen for study. Our results demonstrate that apart from the influence by the formation of clay minerals that drive the saprolite heavier during silicate weathering process, the pedogenic carbonates might have an important influence on the Mg isotopic behavior.

2. Site description and sample collection

The saprolites we study here were developed on early Yanshanian granitoid complex in the Jiangxi province in southeast China. The region has a humid subtropical climate, with a mean annual temperature of 11.6–19.6 °C, and mean annual precipitation of around 1600 mm. The studied region has well-developed vegetation in a subtropical moist rainy climate.

The saprolite exposed here is 10 m in total thickness and consists of an uninterrupted progression from unaltered granites to a highly weathered residue towards the surface (Fig. 1). The granitoid complex is reported as an A-type granite, composed of a K-feldspar granite and accompanying syenite. The Rb–Sr isochron age of this K-feldspar granite is 178.2 ± 0.84 Ma (Fan and Chen, 2000). The unaltered granite contains 27% of plagioclase, and 22% of K-feldspar, 24% of quartz and 8% of mica (Liu et al., 2016); The saprolites are dominated by quartz, ranging from 26% to 90%, and K-feldspar is equally important in lower saprolite. Kaolinite and gibbsite are the main secondary minerals in the profiles, with kaolinite dominant (the content ranging from 4 wt% to 10 wt%, Liu et al., 2016). Fresh saprolite samples were collected along a vertical profile and analyzed for density, clay mineral proportions and bulk composition. In addition, unaltered granite samples were collected from 12 m below.

3. Analytical methods

Concentrations of major elements for all samples were measured using X-ray fluorescence, with precision of better than 2%. Trace elemental concentrations were analyzed by a Finnigan MAT Element ICP-MS after digestion with a HNO_3-HF mixture. the analytic precision is better than 5% (Zhang et al., 2015). Exchangeable cations were replaced by Ammonium Acetate (1 M NH_4-AC, at pH 7). To quantitatively evaluate the relative depletion or enrichment of an element during chemical weathering, the behavior of cations during soil formation can be quantified by normalizing to immobile elements such as Ti, which is demonstrated to be uniformly distributed in all samples (Nesbitt, 1979). Cation (Al, Fe, K and Mg) variations in relation to Ti have been calculated using the following equation in order to evaluate the mobility of element relative to Ti:

$(X)_{norm} = (C_j/C_{Ti})_s /(C_j/C_{Ti})_p$, where C_j and C_{Ti} represent the concentration of element j and Ti, respectively, and "s''and "p'' refer to saprolite and parent rock.

For magnesium isotopic analyses, approximately 50 mg of rock powder was dissolved in Savillex screw-top beakers in a mixture of concentrated HF-HNO_3-HCl. The capped beakers were heated for ~ 48 h at 120 °C on a hot plate in a laminar flow hood. The solutions were then dried, refluxed twice in concentrated HNO_3, then dried again. The dried residue was dissolved in 0.2 ml of 1 N HNO_3 prepared for column separation. Separation of Mg was achieved by cation exchange chromatography with Bio-Rad 200–400 mesh AG50W-X8 resin in 1 N HNO_3 media. The resin beds were cleaned by flushing the columns with 5 ml of 6 M HCl followed by 5 ml Mili-Q water before sample loading. Samples containing ~ 5 μg of Mg were loaded on the resin and eluted by 1 N HNO_3 with Mg yield close to 100%. All samples were passed through at least two cation exchange columns in order to get a pure Mg solution for mass spectrometry measurement.

Mg isotope ratios were measured by MC-ICP-MS (Neptune Instruments) using the standard–sample bracketing (SSB) method in the State Key Laboratory of Loess and Quaternary Geology. Results were reported as δ^{26}Mg and δ^{25}Mg using the DSM3 as standard. Following the above chemical procedure and measuring methods, SRM980 and BCR-1 were analyzed. Results for these solution and rock standards also agree with previously published data (Young and Galy, 2004; Liu et al., 2014) (Table 1). Based on repeated analyses of standards, the external precision of the above isotopic measurement is better than ± 0.06‰.

4. Result

4.1. Elemental and Mg isotopic compositions of the granite regolith

The chemical composition (weight % oxide) of the parental granite in the study site is 73.8% SiO_2, 13.0% Al_2O_3, 0.2% TiO_2, 0.04% P_2O_5, 2.6% Fe_2O_T, 5.0% K_2O, 0.8% CaO, 0.2% MgO, 3.2% Na_2O and 0.1% MnO. Wherein, the MgO content is significantly lower than that in basalt

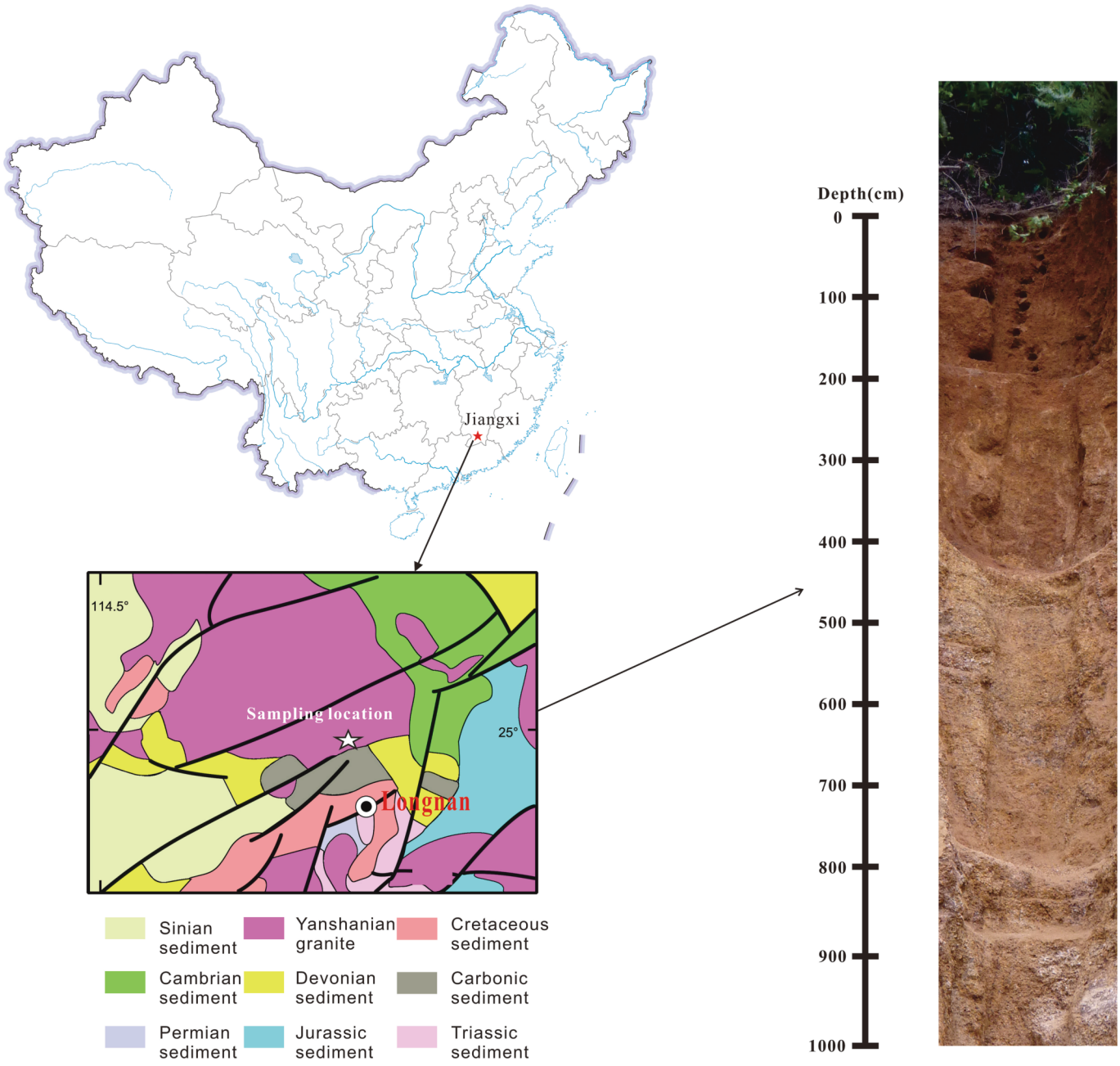

Fig. 1. Location of the sampling site of granite weathering profile in Longnan county, Jiangxi province.

(5 ~ 7.34%, Huang et al., 2012; Liu et al., 2014). Saprolites have much lower MgO contents ranging from 28% to 49% (normalized to Ti, Table 1) relative to parental rock, indicating that about 51% to 72% Mg in the parent rock has been leached from the profile. Mg displays a concentration discontinuity at 310 cm depth in the weathering profile. Above the 310 cm depth, Mg concentrations exhibit decreasing trend towards surface above 75 cm, while it is more or less constant at ~ 0.40 (normalized to Ti) between 75 and 310 cm. Below 310 cm, Mg concentrations gradually become more negative and less variable. This trend is similar to that of FeO_T (Fig. 2). The concentrations of exchangeable Mg of soils are lower, ranging from 0.4 to 1.6 mmol/mg, constituting only between 1% and 7% of the bulk Mg. It also displays highly variable, with its peak values occurring at the surface and the depths of 95 cm and 310 ~ 320 cm.

The parental granite has δ^{26}Mg value around -0.42 ± 0.02‰, which falls out the range of published δ^{26}Mg values of 19 A-type granites from northeastern China (-0.28 to + 0.34‰, Li et al., 2010) but is similar to that found by Li et al. (2021) in the neighbor site of the present study and the Mg isotope composition of andesite (Opfergelt et al., 2012), suggesting the heterogeneous in Mg isotopic composition of the upper continental crust. With one exception at 310 cm depth, the overlying saprolite is much more positive and variable with δ^{26}Mg ranging from -0.37‰~0.27‰ relative to the unaltered granite. Overall, Mg isotopic composition does not vary systematically with depth. The sallowest saprolites have the heaviest isotopic composition while the saprolites at the bottom have the lightest isotopic composition closed to the bedrock.

4.2. *Bedrock-normalized REE patterns of the regolith*

In the profile, normalized REEs show a progressively enrichment in REEs towards the deeper horizons, with the most enrichment at depths around 310 ~ 320 cm. Most of REE are depleted at the surface depths (0

Table 1
Major, trace element concentration, and Mg isotopic composition of saprolite, and unaltered granite; and reference materials analyzed in this study.

Sample	Depth (cm)	MgO (wt.%)	$Mg_{exchange}$ (mmol/kg)	FeO_T (wt.%)	TiO_2 (wt.%)	MgO(norm)	CIA	REE_S (mg/g)	$\delta^{26}Mg$ (‰)	2SD	$\delta^{25}Mg$ (‰)	2SD
JLN-S1-01	10	0.13	1.60	4.17	0.37	0.39	88.01	0.55	0.04	0.07	0.02	0.06
JLN-S1-03	35	0.17	0.50	5.82	0.43	0.44	91.98	0.31	0.09	0.08	0.05	0.05
JLN-S1-04	45	0.14	0.60	4.85	0.35	0.45	92.44	0.32	0.11	0.05	0.06	0.01
JLN-S1-05	55	0.13	0.70	4.30	0.31	0.49	92.25	0.34	0.12	0.09	0.06	0.03
JLN-S1-07	75	0.10	1.30	3.44	0.24	0.48	92.42	0.36	0.08	0.12	0.05	0.05
JLN-S1-09	95	0.09	1.60	3.05	0.22	0.44	91.84	0.39	0.17	0.07	0.08	0.00
JLN-S1-11	115	0.09	0.40	3.21	0.24	0.42	90.72	0.44	−0.25	0.02	−0.13	0.02
JLN-S1-13	135	0.08	0.40	3.00	0.23	0.41	90.15	0.42	0.22	0.04	0.09	0.09
JLN-S1-17	175	0.04	0.70	1.51	0.11	0.40	89.09	0.34	−0.10	0.01	−0.06	0.01
JLN-S1-18	185	0.06	0.60	1.98	0.15	0.42	88.67	0.32	0.17	0.07	0.07	0.07
JLN-S1-19	195	0.08	0.50	2.75	0.21	0.40	86.62	0.57	0.16	0.08	0.07	0.07
JLN-S1-20	210	0.09	0.50	3.24	0.25	0.40	86.99	0.75	−0.16	0.04	−0.04	0.03
JLN-S1-21	230	0.06	0.70	2.12	0.16	0.40	84.99	0.55	0.19	0.22	0.11	0.13
JLN-S1-23	270	0.08	0.60	3.17	0.24	0.38	83.71	0.1	0.15	0.07	0.05	0.08
JLN-S1-24	290	0.09	0.96	3.37	0.27	0.38	84.81	0.99	−0.16	0.09	−0.09	0.02
JLN-S1-25	310	0.10	1.60	3.37	0.27	0.42	83.49	1.35	−0.53	0.18	−0.29	0.08
JLN-S1-26	330	0.10	1.65	3.36	0.26	0.42	81.43	1.43	0.12	0.05	0.06	0.03
JLN-S1-28	370	0.07	0.65	2.94	0.29	0.28	74.56	0.82	0.27	0.06	0.15	0.12
JLN-S1-30	410	0.08	0.74	3.04	0.30	0.29	72.13	0.91	−0.03	0.04	−0.02	0.05
JLN-S1-33	470	0.08	0.49	3.26	0.28	0.34	72.23	0.96	0.11	0.09	0.04	0.01
JLN-S1-37	570	0.07	0.77	2.45	0.26	0.29	69.80	0.88	0.27	0.01	0.11	0.07
JLN-S1-41	650	0.07	0.80	2.58	0.21	0.36	66.58	0.73	−0.37	0.02	−0.18	0.04
JLN-S1-44	710	0.07	0.85	2.73	0.23	0.37	61.64	1.02	−0.18	0.24	−0.07	0.19
Bedrock1									−0.40	0.09	−0.23	0.10
Bedrock2									−0.44	0.12	−0.22	0.06
BCR-1									−0.21	0.12	−0.11	0.04
SRM980									−3.35	0.12	−1.74	0.02

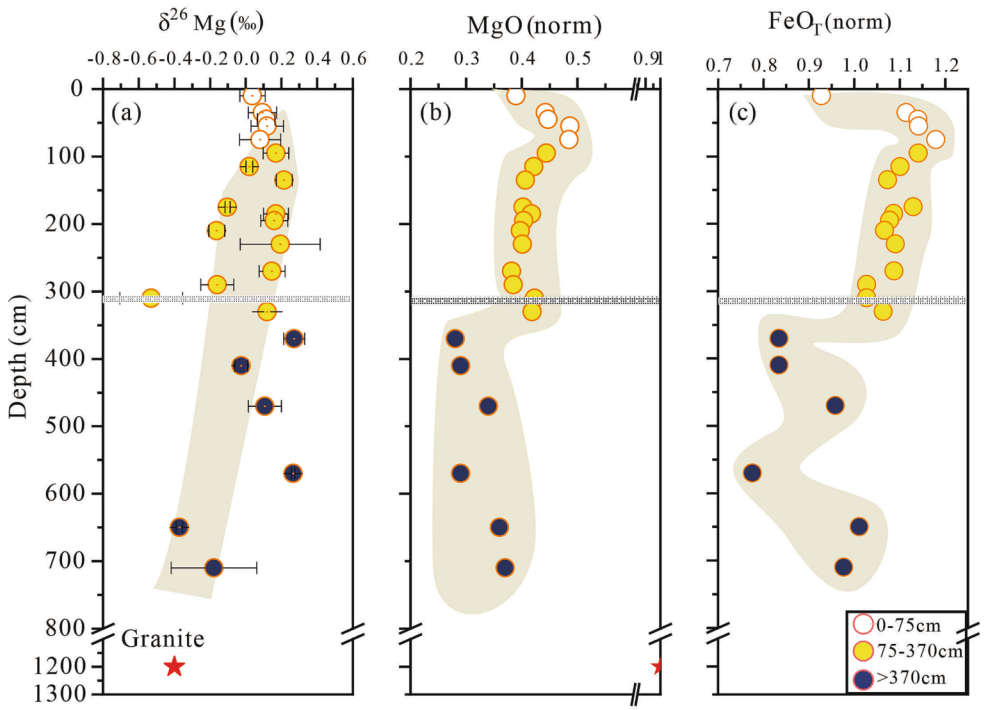

Fig. 2. Magnesium and Iron concentration normalized to titanium, and $\delta^{26}Mg$ of saprolites as a function of depth for the granite weathering profile. The gray line represents the soil horizon at depth of 310 cm.

to115 cm) (Fig. 3). In comparison, the Ce in deeper regolith (below 370 cm) show nearly constant with depth. Cerium anomalies are more variable in the surface than that in the deeper profile (Fig. 3). The larger variation in Ce(norm) values in the upper profile likely reflects stronger redox fluctuations, a consequence of more variation in water saturation, O_2 contents and organic matter (Zhang et al., 2015).

5. Discussion

5.1. Variations of Mg and REE_S concentrations in the profile

Magnesium is fluid-mobile and can be easily leached into the solution during mineral weathering, while the remaining is retained in soils. Like most alkali cations, Mg is depleted in all soil horizons as show in the Fig. 2, indicating net loss of Mg during weathering. In soils, Mg is

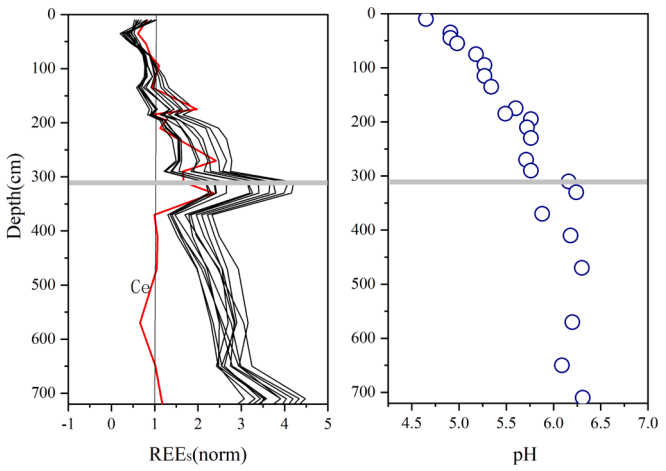

Fig. 3. Variations in REE and pH as a function of depth for the granite weathering profile. The gray line represents the horizon at depth of 310 cm.

distributed between primary minerals, secondary phases, and exchangeable Mg retained on the soil exchange complex (Opfergelt et al., 2014). Previous studies have shown that there were good correlations between the abundance of clay minerals and the concentration of MgO (Huang et al., 2012; Opfergelt et al., 2012). These correlations reflect clay minerals are the main Mg reservoir in the silicate weathering profile. The relatively high abundance of clay minerals in the upper profile may be responsible for the relative enrichment of Mg with the exception of the uppermost sample that is characterized with lower pH. In addition, biological cycling of Mg has the potential to re-distributing Mg in the saprolites because Mg is an important nutrient of plant. During mineral weathering process, the Mg^{2+} cation, released from minerals into soil solutions, can be taken up by roots and stored in vegetation over short (month) or longer (hundreds of years) periods. Magnesium in plants ultimately returns to soils through litterfall decomposition. The lower Mg concentration near the surface can also be attributed to the plant cycling. In the surface soil, the MgO concentration displays remarkable negative correlation with TOC (Fig. 4a). This might reflect that the dilution by the relative low Mg-bearing organic or the leaching with organic-ligand. Compared to the systematic increase with depth above 75 cm, the Mg content between 75 and 310 cm in depth nearly has uniform and relatively low values. This might reflect the reaction balance between leaching and adsorption. However, in the deep profile between 370 cm and 720 cm in depth, the Mg content is the lowest of all the samples, which are owing to the predominant process of leaching in the primary stage of weathering.

REE_S mobilization and redistribution in soil profiles is controlled by regolith production, mineral dissolution, secondary mineral precipitation, and adsorption, which are related to the physicochemical parameters, such as pH, Eh. Overall, the REEs in the profile behave similarly to one another, except for Ce, especially at the depth below 370 cm (Fig. 3). There is a good relationship between REEs and pH (Liu et al., 2022). Particularly, the concentration peak occurs at the depth of 310 cm, where a sharp increase of pH was also observed (Fig. 3). This rise in soil pH would have favored REE adsorption on clay minerals (Lara et al., 2018), especially on kaolinite, for which the cation exchange capacity is dominated by pH-dependent negatively charged sites from broken bonds and lattice defects (Li et al., 2020). In addition, most metals have sorption edges between pH 4 and 6 (Lara et al., 2018), the same range was observed in the profile. This in part explain the enrichment of REE in the profile. In addition to pH effects, depletion-enrichment profiles of metals have also been attributed to chelation by organic ligands in the surface layers of regolith, followed by eluviation and precipitation at lower depths where organic ligands are less abundant (Atkinson and Wright, 1957). However, soil organic carbon (TOC) varies between 0.12 and 3.93 wt%, and is very low (<0.3%) below about 70 cm, therefore eluviation of ligand-bound REE is unlikely to reach the depths of the strongly enrichment at about 310 cm depth before the ligands are scavenged. Otherwise, due to the similarity of REE^{3+} and Ca^{2+} ionic radius, REEs are then easily incorporated into carbonate minerals (Laveuf and Cornu, 2009). In summary, our work highlights pH determines the translocation of trace elements throughout deep regolith profiles, and the fate of trace elements is modulated by a chelation by organic ligands, sorption, and precipitation processes.

5.2. Controls on variation of Mg isotopic composition in saprolite

In this section, we will discuss the behavior of Mg isotopes during granite weathering. The variations in Mg concentration and Mg isotopic composition in this weathering profile likely reflect the reaction balance between dissolution of primary minerals and secondary minerals formation which preferentially absorb heavier or lighter isotope, depending on the mineral-specific.

5.2.1. Effects of external inputs and biogeochemical processes

In the upper profile (<75 cm depth), inflections in the depth profile trends of several geochemical parameters occur. Specifically, the $\delta^{26}Mg$ values and bulk soil Mg concentration show a decreasing trend toward the surface. These concurring variations observed in chemical composition near the surface can be explained either by external atmospheric input or biological recycling. Measurements reported in the literature from other globally distributed sites consistently show negative $\delta^{26}Mg$ values for rainwaters ranging from −1.73 to −0.59‰ (Bolou-Bi et al., 2022 and references therein), which is much lower than those of the top soils in the studied profile. In addition, one local rain water was collected, but in which Mg was not detected. Considering very low Mg concentration and negative $\delta^{26}Mg$ values for rainwater, we can reasonably assume that external inputs is minor. This conclusion is consistent with the study by Li et al. (2021) carried out in a nearby site.

As discussed early, recycling of nutrients by vegetation can modify the soil composition and act as an important role in the material migration in the vertical profiles. Bolou-Bi et al. (2012) reported litterfall can return about 0.90 kg $ha^{-1}year^{-1}$ of Mg to the soil. During these process, soil organic matter produced, which formed chelate with Fe in the upper horizons and subsequently leached and deposited as amorphous material in the deeper horizons (Bolou-Bi et al., 2012). In present study, we observed an enrichment of Fe content in the profile between 75 cm and 310 cm, and a strong positive covariation between bulk Fe concentration and Mg concentration was found (Fig. 5). Although $\delta^{26}Mg$ values of plant tissues have not been measured in present study, measurements reported in previous studies both experimental studies and field investigations showed consistently conclusions that plant tissues is enriched in isotopically light Mg, analyzed $\delta^{26}Mg$ values ranging from −1.36 to −0.18‰ (Bolou-Bi et al., 2010; Opfergelt et al., 2014; Ma et al., 2015; Schuessler et al., 2018). Based on this conclusion, it is reasonable to attribute the change in Mg isotopic composition to litter leaching or litter remineralization in the upper soil. Furthermore, there is a moderate negative covariation between soil TOC and $\delta^{26}Mg$ values (Fig. 4), which suggests that the more input from plant litter, the much lower $\delta^{26}Mg$ values of regolith displays. Given the Mg concentrations of organic matter (leaf litter: average1725 μg Mg g-1C, Herndon, 2012), only 0.007 wt% Mg in the top soil can be associated with organic matter, accounting for 5% of the total Mg. With the assumption that the litter fall is characterized by the Mg isotopic composition with −0.67‰ (Bolou-Bi et al., 2012), it is reasonable to explain the variation of 0.08‰ in the surface soil. Further, the good relationship between the amount of exchangeable Mg (Mg_{exch}) and $\delta^{26}Mg$ values could suggest that plant-related Mg recycling causes the enrichment of light Mg isotopes in the exchangeable Mg pool (Ryu et al., 2020). Summarily, though the $\delta^{26}Mg$ variation in the upper profile is small, it could not exclude the influence from biogeochemical processes. More investigations are needed to

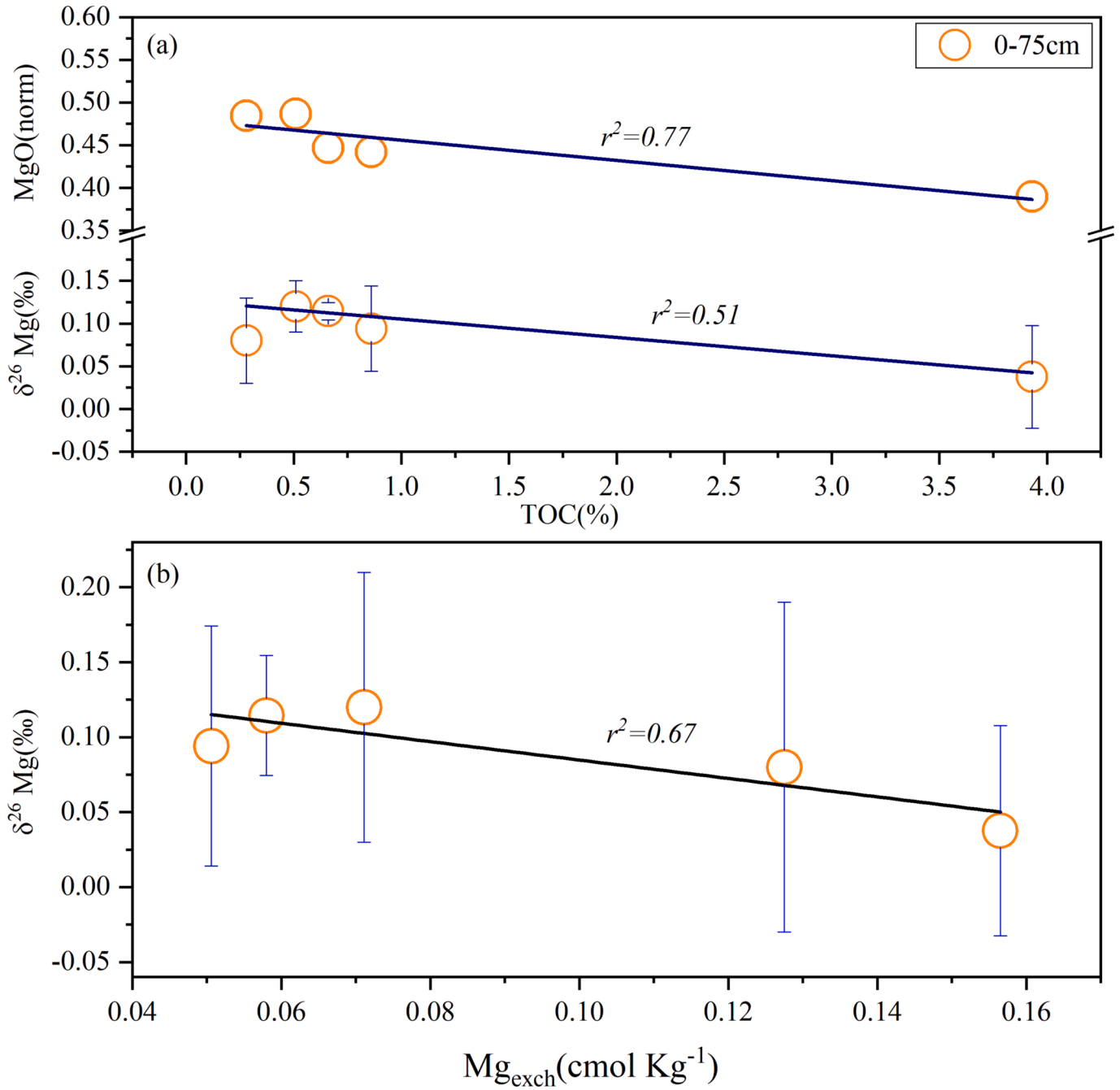

Fig. 4. Variation of δ^{26}Mg and MgO with the abundance of TOC(a), and Variation of δ^{26}Mg with the amount of exchange Mg (b), for upper profile.

quantify more precisely Mg isotope fractionation by biological Mg recycling in the soil system. The narrow δ^{26}Mg variation but significant Mg concentration change could suggest that large concentration of Mg supplied by congruent granite weathering buffers the effect of Mg isotope fractionation by plants (Ryu et al., 2020).

5.2.2. Effects of chemical weathering

Most previous studies have showed that saprolite was generally enriched in ^{26}Mg relative to parental silicate rock indicating that light Mg isotope prefer fluid to solid phase during rock weathering (Teng et al., 2010; Tipper et al., 2010; Huang et al., 2012; Opfergelt et al., 2014; Lara et al., 2017). Expectedly, a similar phenomenon is observed in our studied profile. As showed in Fig. 2, with the exception of one sample at 310 cm horizon, all samples are systemically enriched in ^{26}Mg compared to the granite, with $\Delta^{26}Mg_{regolith\text{-}bedrock} = 0.03 \sim 0.67‰$. The ^{26}Mg enrichment in weathering residue implies that a corresponding fluid depleted in ^{26}Mg should be expected, which is consistent with the observation that rivers draining granitic basin were enriched in lighter Mg isotope (Tipper et al., 2012). The Mg isotopic fractionation during rock weathering is suggested to be caused by two different processes: differential dissolution of isotopically distinct phases or preferentially incorporation heavier Mg isotope by secondary mineral formation (Wimpenny et al., 2010; Ryu et al., 2011, 2016; Tipper et al., 2012).

The preferential dissolution of mineral phases enriched in light Mg isotope have potential to drive the weathering residue isotopically heavier. In present study, the most possible isotopically lighter Mg-rich minerals in granite rock is chlorite. Ryu et al. (2011) reported chlorite has high proportion of Mg up to 141384 ppm and δ^{26}Mg values of which can be as low as −1.82‰. Our study has found that it comprised up to 6% of the total mineral of parental rock (Liu et al., 2016). Accordingly,

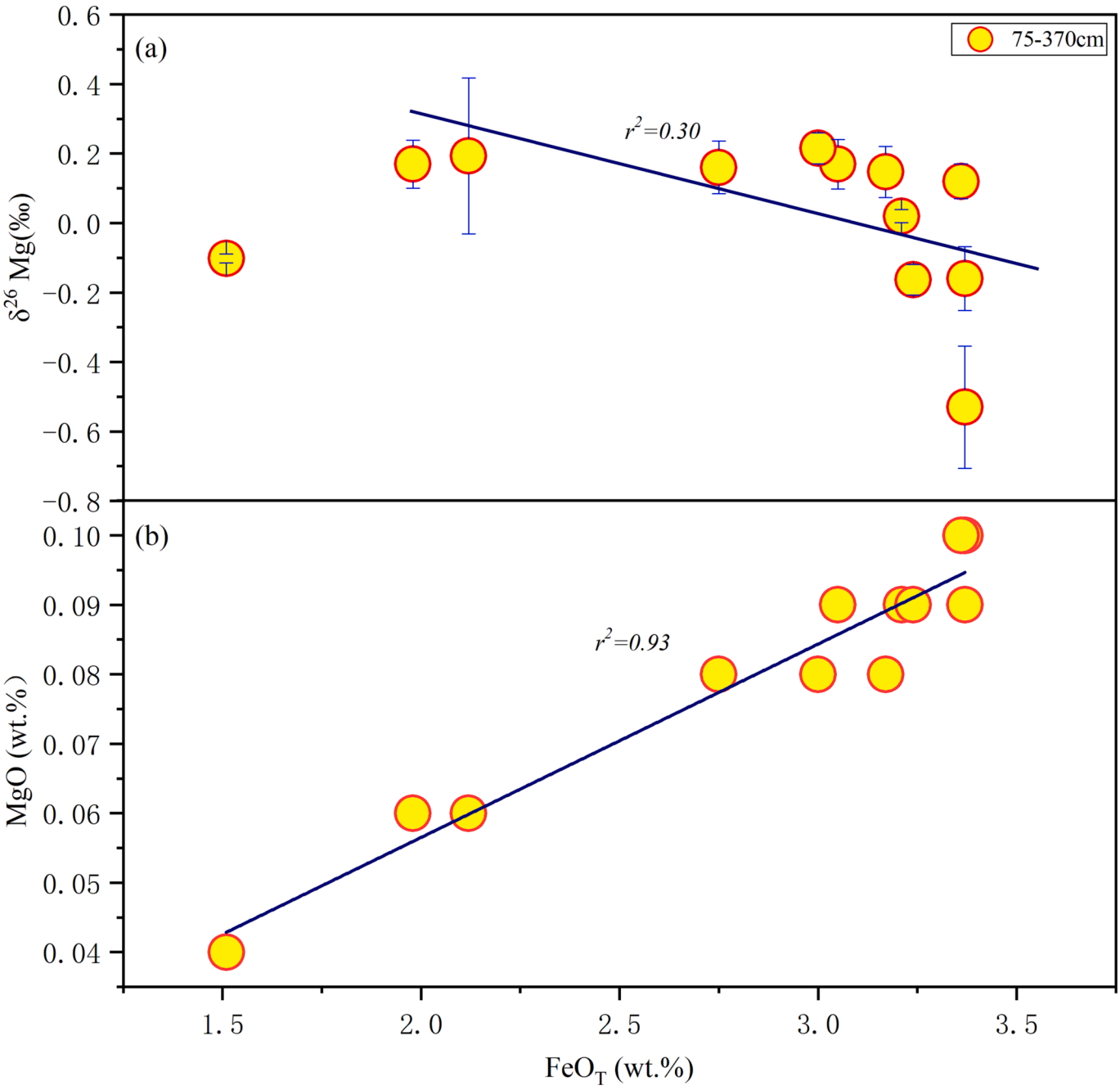

Fig. 5. Variation of δ^{26}Mg (a) and MgO content (wt.%) (b) with FeO_T content (wt.%) for samples at depths between 75 cm and 370 cm.

we can gain a saprolite characterized by −0.31‰ in δ^{26}Mg, with the assumption that the chlorite is characterized by −1.82 ‰ in δ^{26}Mg and all dissolved out. This value is somewhat lighter than that observed in this saprolite for most samples. Moreover, chlorite displays non-systemically decrease with depth in the profile. And no correlation between δ^{26}Mg and the abundance of chlorite in regolith is observed. In addition, another study reported that chlorite was enriched in heavy Mg isotope with an average δ^{26}Mg of + 0.19 ± 0.08‰ (Lara et al., 2017). This isotopically heavy Mg was consistent with the observation that saprock with abundance chlorite was enriched in ^{26}Mg in a granite weathering profile (Li et al., 2021). Consequently, Mg isotopic fractionation associated with primary mineral incongruent dissolution is unlikely to be responsible for the Mg isotope behavior observed in this study.

As a predominant Mg-rich secondary clay mineral derived from progressive weathering of silicates material, kaolinite is present in all samples, representing between 60 and 70% of the clay minerals (Liu et al., 2016). It is the typical product of intensive weathering of feldspar in tropical and sub-tropical areas (Liu et al., 2016). Moreover, many previous studies have demonstrated that kaolinite significantly affect the Mg budget and Mg isotope behavior during silicate weathering (Teng et al., 2010; Huang et al., 2012). In incipient weathering stage, ^{26}Mg may be preferentially incorporated into structures of kaolinite, then driving the soil heavy (Teng et al., 2010; Huang et al., 2012; Ryu et al.,2020). This suggests that kaolinite is likely to exert a significant control on Mg isotope in the profile investigated here. Indeed, there is a generally increase in kaolinite from the bottom to the depth at 400 cm depth, while the trend has not been observed in the upper profile as reported by Liu et al. (2016). The δ^{26}Mg values in the deep profile show a moderately positive correlation with the abundance of kaolinite,

similar to the result reported in a basaltic profile (Huang et al., 2012), while no correlation is observed in the upper profile. Further, apart from the existence of kaolinite, gibbsite also occurs in most of the samples. Gibbsite contents generally rise from 0 wt% at the bottom to 3 wt% at the top of the saprolite. Liu et al. (2014) found that gibbsite preferentially sorb the heavy Mg isotopes, leading to the extreme Mg isotope fractionation. It is noteworthy that the occasional anomalously high gibbsite content at depths of about 370 cm and 570 cm is in correspondence to the highest δ^{26}Mg values. Moreover, in comparison to the relationship between δ^{26}Mg values and the abundance of kaolinite, there is a much stronger correlation between δ^{26}Mg values and kaolinite + gibbsite content in the deep profile (Fig. 6). Hence, the influence of gibbsite is also important. This indicates that incorporation of Mg into the octahedral sites of crystalline secondary minerals (i.e., kaolinite/gibbsite) is partly controlling the soil Mg isotopic composition and this process favors an isotope fractionation towards heavy Mg isotopes (Ryu et al.,2020). Such difference of δ^{26}Mg characteristic between the deep and upper profile might be explained by the transformation of secondary minerals as weathering progressed (Trostle et al., 2013; Ryu et al., 2020). Meanwhile, other processes such as sorption/desorption and precipitation/dissolution, can occur in different weathering stages, which act as different roles with different minerals. For example, as a common natural mineral in soils, Fe oxides can concentrate and control the distribution and mobility of metals or macronutrient in soils (Zhang et al., 2021) and are thus considered to play a key role in the soil environmental behavior of metals, including Mg. Compared to the influence of clay minerals, Fe oxides were found to considerably lower the granite soil δ^{26}Mg values (Gao et al., 2018). As expected, there is a strong positive covariation between MgO and FeO_T concentration at depths between 75 and 370 cm (Fig. 5) in the studied profile. And the moderate correlation between FeO_T and δ^{26}Mg values is found with the exception of two deviation point. This suggests that lighter Mg is preferentially incorporated into Fe oxides phases, which is similar to the behavior of allophane in a basaltic soil (Pogge von Strandmann et al., 2008).

Overall, δ^{26}Mg variation in the studied profile is predominantly controlled by dissolution of primary minerals, during which lighter Mg is preferentially leached, and secondary minerals formation (e.g, kaolinite, gibbsite and Fe oxides) could be also significant.

The chemical index of alteration (CIA) has been widely used to estimate the weathering intensity. The δ^{26}Mg values of saprolite positively correlate with their CIA values, especially in deep profile (Fig. 7). The inverse correlation between δ^{26}Mg and MgO concentration was also observed in the present profile similar to that reported by Li et al. (2020), as well as with the behavior of Mg during saprolite formation in the context of diabase weathering (Teng et al., 2010). Both the increase in δ^{26}Mg and CIA is related to the dissolution of primary minerals and formation of secondary clay minerals during chemical weathering, with preferential enrichment of heavier Mg isotopes in saprolite that has undergone more intense weathering (i.e., higher CIA value) as discussed above.

The Mg loss can be modeled by Rayleigh distillation with one exception at 310 cm depth, with light Mg isotopes preferring fluids to saprolites and with various apparent fractionation factors between saprolite and fluid [$\alpha=(^{26}Mg/^{24}Mg)_{saprolite}/(^{26}Mg/^{24}Mg)_{fluid}$] (Fig. 7). The apparent α value vary from 1.0002 to 1.001 (Fig. 7), which falls in the range of observed values during the weathering of basalt (Huang et al., 2012) corresponding to a change of Mg isotope fractionation between saprolite and fluid from 0.05‰ up to 0.4‰ accompanied by 50 ~ 80% Mg loss. The large range in α values, especially for the upper profiles, reflects apart from the weathering processes, additional processes is needed to explain such high α values, such as adsorption/desorption, dissolution/precipitation and so on.

5.2.3. *Explanation on the light Mg isotopic composition*

In the present weathering profile, the lowest δ^{26}Mg value of −0.53‰ measured in bulk saprolite at about 310 cm depth, is slightly lighter than the parental granite (-0.42 ‰) but much lighter than the other saprolite samples. Therefore, the data for this sample cannot be explained solely by the weathering reaction explained above, implying an additional sources or processes occurring.

Firstly, we can exclude the contribution of light Mg from primary minerals based on the absence of most possible ^{24}Mg-enriched mineral (chlorite) in the isotopic excursion. Apart from this, two alternative mechanisms may account for this:1) the accumulation of light Mg isotopes in exchangeable sites of Mg-depleted clay minerals; 2) the contribution of light Mg from carbonates.

5.2.3.1. The accumulation of light Mg isotopes in exchangeable sites of Mg-depleted minerals. Mg retention on the soil exchange complex was demonstrated to a significant Mg pool, which has an important influence on Mg budget and Mg isotope composition in soils. This phase was

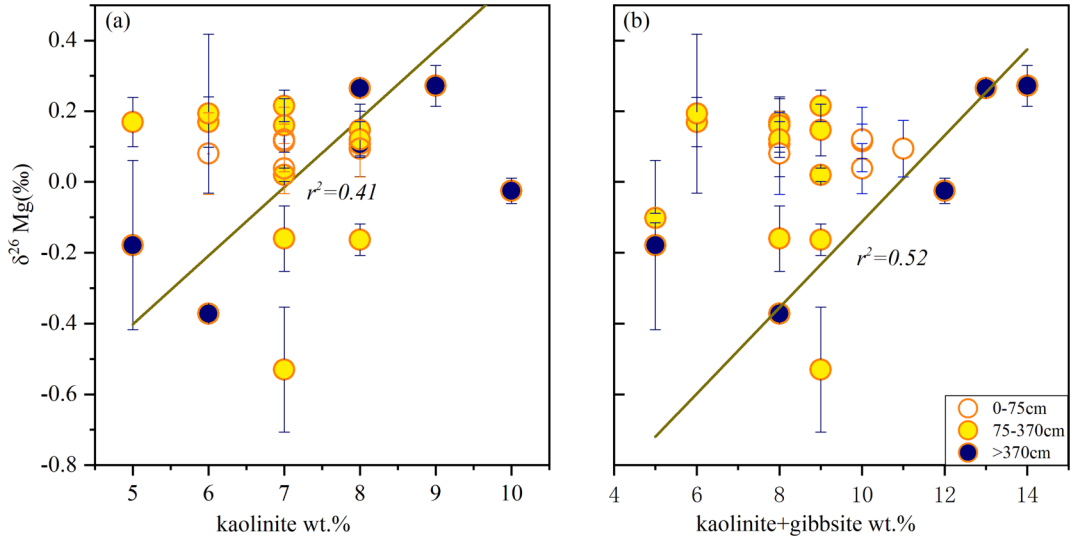

Fig. 6. Variation of δ^{26}Mg of the saprolites with the abundance of kaolinite (a), and kaolinite and gibbsite for the granite weathering profile (b). open circles represent samples at or above 75 cm depth, and closed yellow circles are samples between 75 cm and 370 cm, and closed blue circles below 370 cm. The regression lines are based on the samples at depth below 370 cm. (For interpretation of the references to colour in this figure legend, the reader is referred to the web version of this article.)

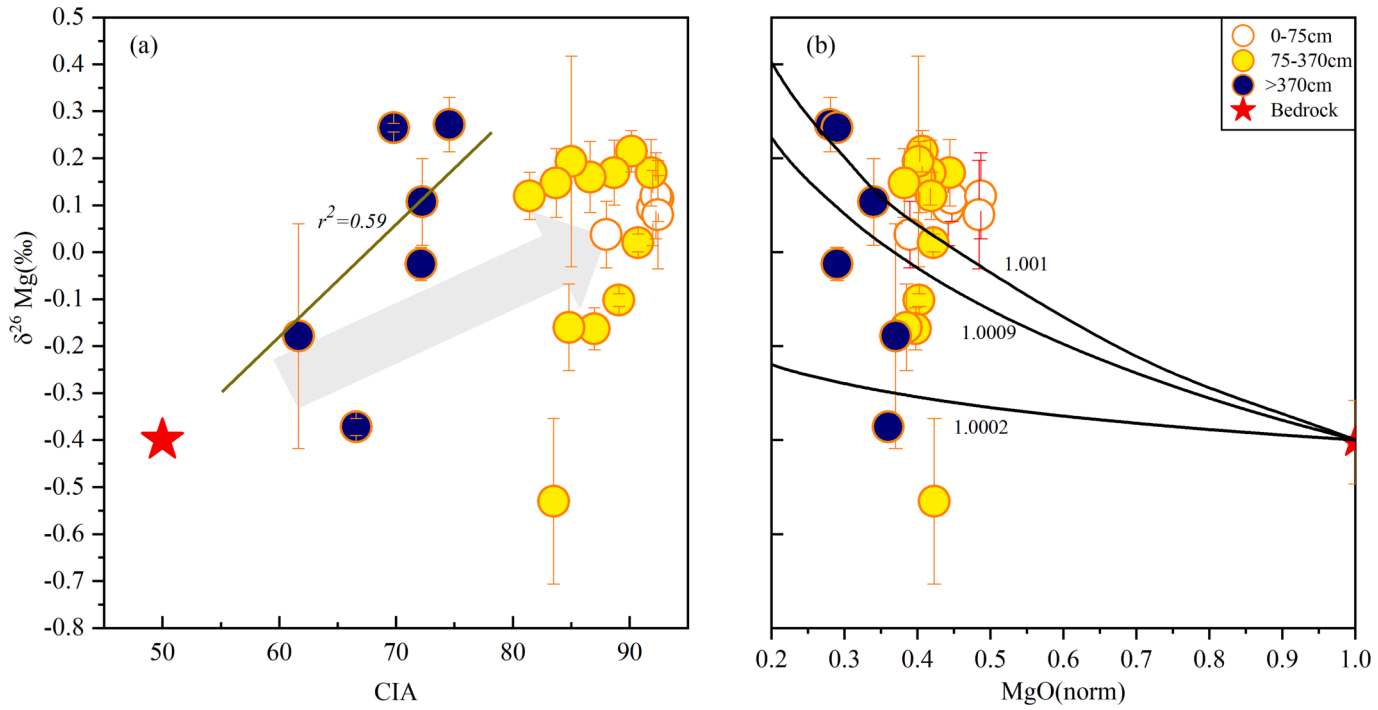

Fig. 7. Variation of the δ^{26}Mg of the bulk regolith with the CIA values. The regression line is based on the samples at depth below 370 cm(a); Magnesium concentration normalized to titanium vs. δ^{26}Mg for saprolite profile (b). Curved lines depict Mg removal via Rayleigh distillation for different values of the fractionation factor α [$\alpha=(^{26}Mg/^{24}Mg)_{saprolite}/(^{26}Mg/^{24}Mg)_{fluid}$]. Rayleigh distillation equation: $\delta^{26}Mg_{saprolite}=(\delta^{26}Mg_{granite}+1000)f^{(\alpha-1)}-1000$; f: the fraction of Mg remaining in the rock, calculated from $Mg_{saprolite}/Mg_{granite}$. The Curved lines are in response to different fractionation factor(b). Star represents unweathered granite; and open circles represent samples at or above 75 cm depth, and closed yellow circles are samples between 75 cm and 370 cm and closed blue circles below 370 cm. Error bars represent 2SD uncertainties. (For interpretation of the references to colour in this figure legend, the reader is referred to the web version of this article.)

generally enriched in light Mg isotope as reported in previous studies (Opfergelt et al., 2012; Opfergelt et al., 2014; Wimpenny et al., 2014; Gao et al., 2018). The data of volcanic soil provided evidence that Mg retained on the soil exchange complex contributed to the shift to lighter Mg isotope compositions in soils (Opfergelt et al., 2012; Opfergelt et al., 2014), as also observed in highly weathered andesitic and basaltic profile (Huang et al., 2012; Ma et al., 2015). Magnesium on the soil exchange complex represents Mg retained by short-range ordered minerals or associated with fresh organic matter (Opfergelt et al., 2012). Huang et al. (2012) and Gao et al. (2018) documented that the soil containing high proportion of kaolinite were characterized by lighter Mg isotope composition relative to parent rock. This is attributed to either preferential adsorption the light Mg isotope as soil exchange phase in the surface of kaolinite or preferential desorption heavy Mg isotope with increasing leaching during weathering. An experimental study also reported that kaolinite has isotopically light δ^{26}Mg values due to containing higher proportions of exchangeable Mg^{2+} (Wimpenny et al., 2014). In present study, however, there is no significant increase of kaolinite abundance in this excursion layer. The influence of desorption heavy Mg isotope by kaolinite minerals also cannot accommodate Mg variation, as the exchange Mg content at the 310 cm depth shows relative higher compared to other soil layers. In addition, in previous studies, the decreasing Mg isotopes associated with the ion exchange processes occurred always in upper profile that no deeper than 200 cm, where extreme weathering occurred, the Mg exchange phase is predominant. However, the sample at our study is in relative deeper profile, there is less likely to have significant amounts of soil exchange complexes. Alternatively, considerable amount of organic matter in the soil and Mg sorption on the organic matter would lead to ^{24}Mg enrichment. Nonetheless, the influence from organic matter is likely limited in this horizon, as TOC is<0.3%.

As discussed in section 5.2.2, Fe oxides characterized by lighter Mg isotopes (-1.79 to −2.15‰, Gao et al., 2018) can also drive the bulk soil δ^{26}Mg to lighter values. Based on this fact, the lower δ^{26}Mg in soil is expected to occur in where the Fe oxyhydroxides is significantly enriched. Whereas the maximum enrichment of Fe oxyhydroxides found at 100 cm depth here did not accumulate light Mg isotope. Otherwise, adsorption of ions onto these secondary minerals strongly depends on the surface charge properties of minerals, which can be described by the pH of the point of zero charge (pH_{pzc}). The pH_{pzc} of Al- and Fe oxyhydroxides is higher, ranging from 6.12 to 8.81 (Marek, 2006). At the pH of saprolite at depth of 310 cm (6.16), the surface charge of Al- and Fe-oxy-hydroxides is neutral. In this case, Mg^{2+}, one of the most common exchangeable cations, is unlikely adsorbed to the surfaces of Fe(III)-(hydr)oxides.

5.2.3.2. The contribution of light Mg from carbonates. The contribution of carbonates is another possible explanation for Mg isotopic variation, as carbonate minerals are an isotopically light reservoir of Mg, as lower as −5.54 ‰ (Higgins and Schrag, 2010), which can lower the soil δ^{26}Mg values. For example, studies on loess showed a negative correlation between δ^{26}Mg values and CaO contents (Huang et al., 2013; Wimpenny et al., 2014), which was explained by carbonate minerals in loess contributing light Mg isotopes to the bulk loess. Similarly, Wang et al. (2015) demonstrated that carbonates in mudrocks caused the bulk rocks to become significantly enriched in isotopically light Mg. In our study, the concurring of marked increase of CaO content and the LOI value in the excursion layer were observed. Though the increase of LOI values can reflect either the increase of carbonates content or the increase of organic matter, however, as discussed above, the contribution of organic matter was excluded. Based on this observation, a significant increase of carbonates is expected in this soil layer. Thereafter the question raised, where did the carbonates originate from? The carbonates can be subdivided into three large groups in regard to its sources: geogenic carbonates, biogenic carbonates and pedogenic carbonates (Zamanian et al., 2016). We will discuss the three possible sources in detail in the

next section.

An experimental study document that the carbonate fraction in granite is characterized by much higher δ^{26}Mg value of −0.73‰ compared to the reported averaged values of carbonates (Ryu et al., 2011), but slightly lighter than the discussed sample. Thus, the presence of minor carbonate in granite weathering product can be responsible for the lower Mg isotopic value. Geogenic carbonates are referred to the phase which have remained or are inherited from soil parent materials such as limestone particles or allocated onto the soil from other locations by calcareous dust or landslides etc. However, in the weathering profile study here, there is no carbonates detected in the parental rock. The contribution inherited from parent rock can thus be excluded. Due to the lighter soil layer located at depth 310 cm, the contribution from dust input is less likely. In light of little influence by biological effect as demonstrated earlier, biogenic carbonates are also impossible at this layer site.

Lastly, pedogenic carbonates is the most possible forms found in our study. As previous studies documented that dissolution of primary minerals generally release isotopically light Mg into soil solution. Accordingly, we speculate that migration of the soil solution with isotopically light Mg downward results in the variation of the δ^{26}Mg values of secondary carbonates. When precipitation is high, the soil solution would move deeper, together with a substantial amount of isotopically light Mg. In the lower part of precipitation-leached layers, secondary carbonates with relatively high Mg concentrations and low δ^{26}Mg values, would be expected to form. The formation of secondary carbonate is likely occurring in soils which are clay-rich and relatively impermeable. Such requirement is matched in the study site.

Trace element chemistry further supports the formation of carbonates. Rare-earth elements (REEs) were thought to have great potential for tracing the formation of pedogenic carbonates. During this process, REEs complex with carbonate ions, then migrate in soil profiles, and ultimately REEs carbonate complexes precipitate when reaching adequate soil pH conditions (Laveuf and Cornu, 2009). Similar to other geochemical parameters in this layer, there is an obvious enrichment of rare-earth elements and accompanied by the increasing of soil pH (Fig. 3). These observations further support that secondary carbonate formation did occur at this layer. Carbonates are also thought to preferentially partitioned to the $>$ 2 mm portion of soil (Trostle, 2013). At the 310 cm horizon, the observation of a sharp increase of large soil grain further supports the presence of carbonates.

We assumed that the Mg in this layer followed simple mixing between the two dominant sources of Mg, magnesium derived from silicates minerals forming during granite weathering and magnesium derived from carbonates precipitated from soil solution. As a first approximation, we use a closed system isotope balance to constrain the isotopic composition of fluids resulting from the decomposition of granite to saprolite at the weathering profile scale:

$$\delta^{26}Mg_{granite} = f\delta^{26}Mg_{saprolite} + (1-f)\delta^{26}Mg_{fluid}$$

with f referring to the mass fraction of Mg remaining in the saprolite, calculated relative to fresh granite. Accordingly, we predict $\delta^{26}Mg_{fluid}$ of −0.69 ‰, which falls in the range of that reported in other studies (Tipper et al., 2010; Pogge von Strandmann et al.,2012; Lara et al.,2017). And the calculated $\Delta^{26}Mg_{calcite\text{-}fluid}$ is −1.62‰, with the assumption that pedogenic carbonates have a δ^{26}Mg value around −2.31‰ similar to that reported in other literatures (Tipper et al., 2006; Trostle, 2013). This value is consistent with the range of Mg isotope fractionation ($\Delta\ ^{26}Mg_{carbonates\text{-}fluid}$ ~ -2.60‰ to.

−1.43‰, Mavromatis et al., 2012, 2014).

Taking into account the Mg pools in soils, simplified as carbonates and non-carbonates phases, and the δ^{26}Mg signatures of these two individual reservoirs, the bulk regolith Mg isotope composition can be recalculated by the following mass balance:

$$\delta^{26}Mg_{regolith} = f\delta^{26}Mg_{car} + (1-f)\delta^{26}Mg_{non-c}$$

in which f is fraction of Mg in the carbonate form, $\delta^{26}Mg_{regolith}$, $\delta^{26}Mg_{car}$ and $\delta^{26}Mg_{non\text{-}c}$ are the δ^{26}Mg values of the regolith, pedogenic carbonates and non-carbonates minerals that mainly represent the granitic weathering product. We can estimate that 22.9% of Mg in this layer presented in carbonates and the remaining 77% in silicate phases.

6. Implications

The Mg budget and Mg isotope geochemistry behavior in the critical zone is mainly controlled by the weathering of igneous rocks. This is related to two processes: primary minerals dissolution and secondary minerals formation. These processes lead to loss of isotopically light Mg from continents, accompanied by the heavy Mg isotope enriched in the weathering residue. However, there is a large variation of the Mg isotope composition in the weathering residue (-0.63 ~ 1.72‰), which highly depend on the mineralogy of the phase as show in Fig. 8. The extremely high δ^{26}Mg value found so far is bauxites in an extremely weathering zone, the formation of gibbsite was thought to account for this (Liu et al., 2014). Kaolinite, illite and chlorite also have the potential to drive the soil toward positive (Huang et al., 2012; Brewer et al., 2018; Li et al., 2021). However, other isotopically lighter Mg bearing minerals such as carbonates display opposite. Our study provides the first evidence that the formation of pedogenic carbonates potentially impacts soil Mg isotope composition in granitic weathering profile, even in subtropical areas with rich rainy, and act as a buffer for soil solution. This can contribute to the heavier riverine signatures in silicate catchments, which could be another explanation for the Mg isotopically heavy rivers draining silicate basin. Such process might lead to overestimation of the contribution from silicate weathering, when discern the weathering budget from different rocks. Further, the data highlight that pedogenic carbonates is likely an important terrestrial C pool stocked in deep soil layers, which might be partly responsible for the “Missing C” in terrestrial. Previous study proposed that the SIC stocked in soil up to 2 m is about 950 Pg C (Zamanian et al., 2016), which shows its great role in the global C cycle. Nevertheless, the data in deeper soils is limited, present study thus imply that Mg isotope has great potential to unveil stocked C in deeper soils.

7. Conclusion

Result for the Mg isotopic composition of the saprolite developed on a granite rock demonstrates that the saprolite is consistently isotopically heavier than the unweathered granitic rock. This result is thus in agreement with the widely held view that continental weathering releases light Mg to the hydrosphere, leaving isotopically heavy Mg behind in the regolith. Magnesium isotope behavior during weathering is related to various processes, and highly depend on the mineralogy of secondary phases**.** The impact of kaolinite and gibbsite, and Fe oxides is significant in the studied profile. The Mg budget in the upper soil is significantly influenced by the biological cycling. The correlation between δ^{26}Mg, and CIA, and MgO in deep profile suggests that large Mg isotope fractionation accompanied by the loss of Mg occurs in the early stage of weathering, and which can be explained by Rayleigh distillation. This difference of δ^{26}Mg characteristic between the deep and upper profile might be explained by the transformation of secondary minerals as weathering advanced, although the respective contribution cannot be concluded by the current data. Moreover, this study provide evidence that pedogenic carbonates in silicate weathering profile have the potential to drive the soil enriched in lighter Mg isotope. Thus, if secondary carbonate is widespread in silicate soils, then the geochemical cycling of Mg in critical zone will need to be reevaluated.

CRediT authorship contribution statement

BaiLing Fan: Data curation, Formal analysis, Investigation, Methodology, Resources, Writing – original draft, Writing – review & editing.

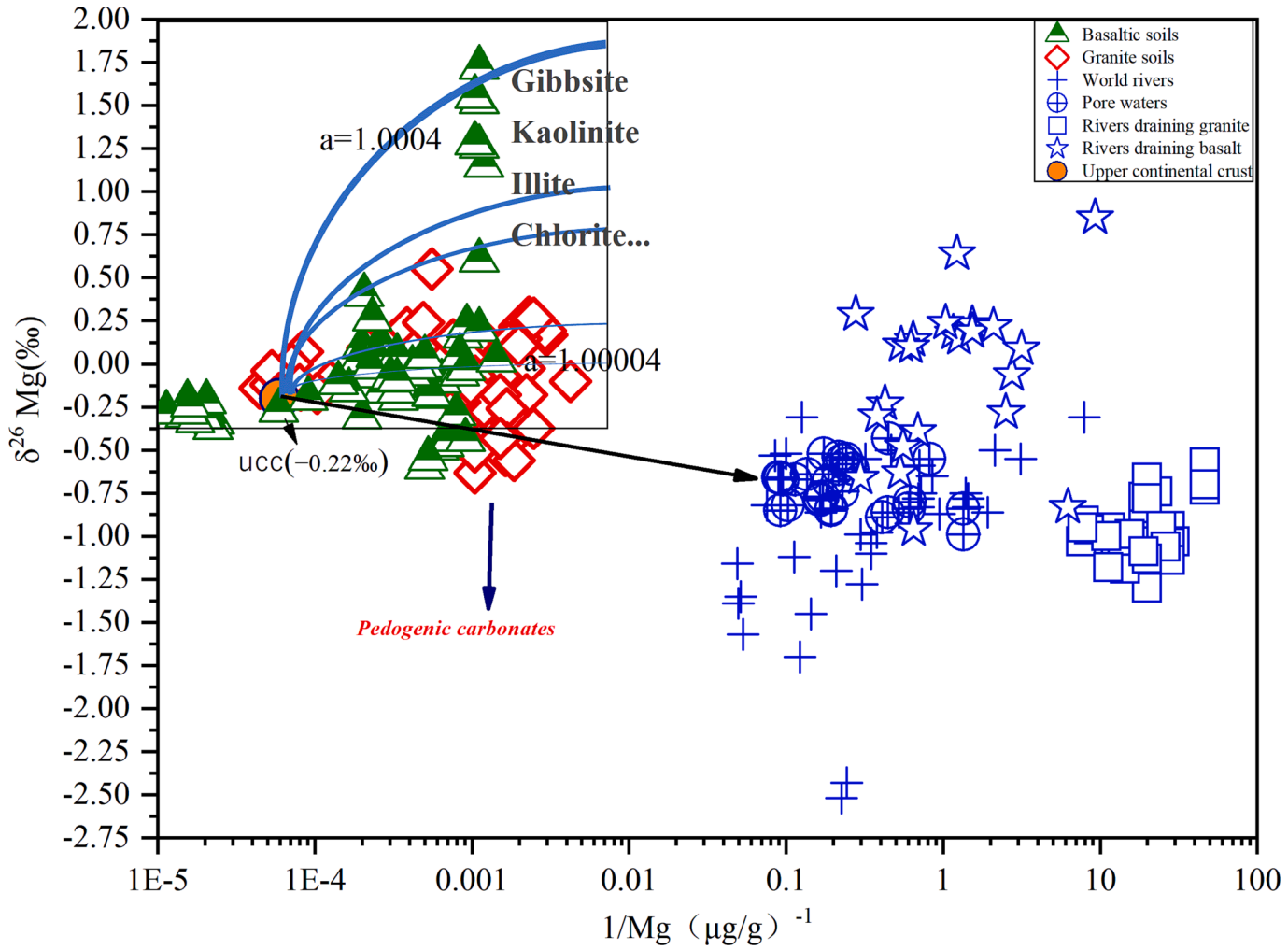

Fig. 8. Relationship between δ^{26}Mg and 1/Mg in weathered products, the data of granite weathering profile from Brewer et al. 2018; Li et al. 2021, and that for basalt from Huang et al.2012; Liu et al.2014, Ryu et al.2020, the data of global river from Tipper et al.2006, pore water from Pogge von Strandmann et al.2012, and rivers draining granite and basalt from Tipper et al.2012, Pogge von Strandmann et al.2008.

XiangQin Yang: Writing – original draft, Writing – review & editing. **Ke Jiang:** Data curation, Software, Validation. **ZhiQi Zhao:** Conceptualization, Funding acquisition, Investigation, Project administration, Resources, Supervision, Validation, Writing – original draft, Writing – review & editing.

Declaration of Competing Interest

The authors declare that they have no known competing financial interests or personal relationships that could have appeared to influence the work reported in this paper.

Data availability

The data that has been used is confidential.

Acknowledgments

This work was funded by National Natural Science Foundation of China (Grant No. 41930863, 42263002, 41130536, 42263007, 42273050), Basic research, Science and Technology Foundation of Guizhou Province, China (grant number: [2019]1155). The authors thank T.Z. Liu, B.J. Liu, Z.J. Zhang and L.F. Cui for collecting the soil samples used in this study. We are thankful for the constructive comments on drafts by K.J. Huang and L.F. Gou.

References

Atkinson, H.J., Wright, J.R., 1957. Chelation and the Vertical Movement of Soil Constituents. Soil Sci. 84, 1–12.
Berner, R.A., Lasaga, A.C., Garrels, R.M., 1983. The carbonate-silicate geochemical cycle and its effect on atmospheric carbon dioxide over the past 100 million years. Am. J. Sci. 283, 641–683.
Black, J.R., Epstein, E., Rains, W.D., Yin, Q.Z., Casey, W.H., 2008. Magnesium-isotope Fractionation During Plant Growth. Environ. Sci. Technol. 42, 7831–7836.
Bolou-Bi, E.B., Poszwa, A., Leyval, C., Vigier, N., 2010. Experimental determination of magnesium isotope fractionation during higher plant growth. Geochim. Cosmochim. Acta. 74, 2523–2537.
Bolou-Bi, E.B., Vigier, N., Poszwa, A., Boudot, J.P., Dambrine, E., 2012. Effects of biogeochemical processes on magnesium isotope variations in a forested catchment in the Vosges Mountains (France). Geochim. Cosmochim. Acta. 87, 341–355.
Bolou-Bi, E.B., Legout, A., Laudon, H., Louvat, P., Pollier, B., Gaillardet, J., Bishop, K., Köhler, S.J., 2022. Use of stable Mg isotope ratios in identifying the base cation sources of stream water in the boreal Krycklan catchment (Sweden). Chem. Geol. 588, 120651.
Brewer, A., Teng, F.Z., Dethier, D., 2018. Magnesium isotope fractionation during granite weathering. Chem. Geol. 501, 95–103.
Fan, C.F., Chen, P.R., 2000. Nd and Sr isotopic compositions of Pitou granitoid in South Jiangxi Province. Contributions to Geology and Mineral Resources Research. 15 (3), 282–287 in Chinese with English Abstract.
Gaillardet, J., Dupré, B., Louvat, P., Allegre, C., 1999. Global silicate weathering and CO_2 consumption rates deduced from the chemistry of large rivers. Chem. Geol. 159, 3–30.
Gao, T., Ke, S., Wang, S.J., Li, F., Liu, C., Lei, J., Liao, C.Z., Wu, F., 2018. Contrasting Mg isotopic compositions between Fe-Mn nodules and surrounding soils: Accumulation of light Mg isotopes by Mg-depleted clay minerals and Fe oxides. Geochim. Cosmochim. Acta. 237, 205–222.

Herndon, E.M., 2012. Biogeochemistry of manganese contamination in a temperate forested watershed. The Pennsylvania State University, PhD diss.
Higgins, J.A., Schrag, D.P., 2010. Constraining magnesium cycling in marine sediments using magnesium isotopes. Geochim. Cosmochim. Acta. 74, 5039–5053.
Hindshaw, R.S., Tosca, R., Tosca, N.J., Tipper, E.T., 2020. Experimental constraints on Mg isotope fractionation during clay formation: Implications for the global biogeochemical cycle of Mg. Earth Planet. Sci. Lett. 531, 115980.
Huang, K.J., Teng, F.Z., Wei, G.J., Ma, J.L., Bao, Z.Y., 2012. Adsorption-and desorption-controlled magnesium isotope fractionation during extreme weathering of basalt in Hainan Island. China. Earth Planet. Sci. Lett. 359, 73–83.
Huang, K.J., Teng, F.Z., Elsenouy, A., Li, W.Y., Bao, Z.Y., 2013. Magnesium isotopic variations in loess: Origins and implications. Earth Planet. Sci. Lett. 374, 60–70.
Jiang, H., Liu, W.J., Xu, Z.F., Zhou, X.D., Zheng, Z.Y., Zhao, T., Zhou, L., Zhang, X., Xu, Y. F., Liu, T.Z., 2018. Chemical weathering of small catchments on the Southeastern Tibetan Plateau I: Water sources, solute sources and weathering rates. Chem. Geol. 500, 159–174.
Lara, M.C., Buss, H.L., Pogge von Strandmann, P.A.E., Schuessler, J.A., Moore, O.W., 2017. The influence of critical zone processes on the Mg isotope budget in a tropical, highly weathered andesitic catchment. Geochim. Cosmochim. Acta. 202, 77–100.
Lara, M.C., Buss, H.L., Pett-Ridge, J.C., 2018. The effects of lithology on trace element and REE behavior during tropical weathering. Chem. Geol. 500, 88–102.
Laveuf, C., Cornu, S., 2009. A review on the potentiality of Rare Earth Elements to trace pedogenetic processes. Geoderma. 154 (1), 1–12.
Li, W.Y., Teng, F.Z., Ke, S., Rudnick, R.L., Gao, S., Wu, F.Y., Chappell, B.W., 2010. Heterogeneous magnesium isotopic composition of the upper continental crust. Geochim. Cosmochim. Acta. 74, 6867–6884.
Li, M., Zhou, M.F., Williams-Jones, A.E., 2020. Controls on the Dynamics of Rare Earth Elements During Subtropical Hillslope Processes and Formation of Regolith-Hosted Deposits. Econ. Geol. 115, 1097–1118.
Li, M., Teng, F.Z., Zhou, M.F., 2021. Phyllosilicate controls on magnesium isotopic fractionation during weathering of granites: Implications for continental weathering and riverine system. Earth Planet. Sci. Lett. 553, 116613.
Liu, W.J., Liu, C.Q., Brantley, S.L., Xu, Z.F., Zhao, T., Liu, T.Z., Yu, C., Xue, D.S., Zhao, Z. Q., Cui, L.F., Zhang, Z.J., Fan, B.L., Gu, X., 2016. Deep weathering along a granite ridgeline in a subtropical climate. Chem. Geol. 427, 17–34.
Liu, W.J., Xu, Z.F., Sun, H.G., Zhao, T., Shi, C., Liu, T.Z., 2018. Geochemistry of the dissolved loads during high-flow season of rivers in the southeastern coastal region of China: anthropogenic impact on chemical weathering and carbon sequestration. Biogeosciences 15 (16), 4955–4971.
Liu, W.J., Li, Y.C., Wang, X., Cui, L.F., Zhao, Z.Q., Liu, C.Q., Xu, Z.F., 2022. Weathering stage and topographic control on rare earth element (REE) behavior: New constraints from a deeply weathered granite hill. Chem. Geol. 610, 121066.
Liu, X.M., Teng, F.Z., Rudnick, R.L., McDonough, W.F., Cummings, M.L., 2014. Massive magnesium depletion and isotope fractionation in weathered basalts. Geochim. Cosmochim. Acta. 135, 336–349.
Liu, W.J., Xu, Z.F., Jiang, H., Zhou, X.D., Zhao, T., Li, Y.C., 2023. Lithological and glacial controls on sulfide weathering and the associated CO_2 budgets in the Tibetan Plateau: New constraints from small catchments. Geochim. Cosmochim. Acta. 343, 341–352.
Ma, L., Teng, F.Z., Jin, L., Ke, S., Yang, W., Gu, H.O., Brantley, Susan.L.,, 2015. Magnesium isotope fractionation during shale weathering in the Shale Hills Critical Zone Observatory: Accumulation of light Mg isotopes in soils by clay mineral transformation. Chem. Geol. 397, 37–50.
Marek, K., 2006. pH-dependent surface charging and points of zero charge: III. Update. J. Colloid Interface Sci. 298, 730–741.
Mavromatis, V., Pearce, C., Shirokova, L.S., Bundeleva, I.A., Pokrovsky, O.S., Benezeth, P., Oelkers, E.H., 2012. Magnesium isotope fractionation during inorganic and cyanobacteria-induced hydrous magnesium carbonate precipitation. Geochim. Cosmochim. Acta. 76, 161–174.
Mavromatis, V., Meister, P., Oelkers, E.H., 2014. Using stable Mg isotopes to distinguish dolomite formation mechanisms: A case study from the Peru Margin. Chem. Geol. 385, 84–91.
Nesbitt, H.W., 1979. Mobility and fractionation of rare earth elements during weathering of a granodiorite. Nature.
Oliva, P., Viers, J., Dupré, B., 2003. Chemical weathering in granitic environments - ScienceDirect. Chem. Geol. 202, 225–256.
Opfergelt, S., Georg, R.B., Delvaux, B., Cabidoche, Y.M., Burton, K.W., Halliday, A.N., 2012. Mechanisms of magnesium isotope fractionation in volcanic soil weathering sequences. Guadeloupe. Earth Planet. Sci. Lett. 341–344, 176–185.
Opfergelt, S., Burton, K.W., Georg, R.B., West, A.J., Guicharnaud, R.A., Sigfusson, B., Siebert, C., Gislason, S.R., Halliday, A.N., 2014. Magnesium retention on the soil exchange complex controlling Mg isotope variations in soils, soil solutions and vegetation in volcanic soils. Iceland. Geochim. Cosmochim. Acta. 125, 110–130.
Oskierski, H.C., Beinlich, A., Mavromatis, V., Altarawneh, M., Dlugogorski, B.Z., 2019. Mg isotope fractionation during continental weathering and low temperature carbonation of ultramafic rocks. Geochim. Cosmochim. Acta. 262, 60–77.
Pogge von Strandmann, P.A.E., Burton, K.W., James, R.H., van Calsteren, P., Gislason, S., 2008. The influence of weathering processes on riverine magnesium isotopes in a basaltic terrain. Earth Planet. Sci. Lett. 276, 187–197.
Pogge von Strandmann, P.A.E., Opfergelt, S., Lai, Y.J., Sigfússon, B., Gislason, S.R., Burton, K.W., 2012. Lithium, magnesium and silicon isotope behaviour accompanying weathering in a basaltic soil and pore water profile in Iceland. Earth Planet. Sci. Lett. 339, 11–23.
Ryu, J.S., Jacobson, A.D., Holmden, C., Lundstrom, C., Zhang, Z.F., 2011. The major ion, $\delta^{44/40}$Ca, $\delta^{44/42}$Ca, and $\delta^{26/24}$Mg geochemistry of granite weathering at pH=1 and T= 25°C: power-law processes and the relative reactivity of minerals. Geochim. Cosmochim. Acta. 75, 6004–6026.
Ryu, J.S., Vigier, N., Decarreau, A., Lee, S.W., Lee, K.S., Song, H., Petit, S., 2016. Experimental investigation of Mg isotope fractionation during mineral dissolution and clay formation. Chem. Geol. 135–145.
Ryu, J.S., Vigier, N., Derry, L., Chadwick, O.A., 2020. Variations of Mg isotope geochemistry in soils over a Hawaiian 4 Myr chronosequence. Geochim. Cosmochim, Acta, p. 292.
Schmitt, A.D., Vigier, N., Lemarchand, D., Millot, R., Stille, P., Chabaux, F., 2012. Processes controlling the stable isotope compositions of Li, B, Mg and Ca in plants, soils and waters: A review. C. R. Geosci. 344, 704–722.
Schuessler, J.A., Friedhelm, V.B., Julien, B., David, U., Tilak, H., 2018. Nutrient cycling in a tropical montane rainforest under a supply-limited weathering regime traced by elemental mass balances and Mg stable isotopes. Chem. Geol. 497, 74–87.
Teng, F.Z., 2017. Magnesium Isotope Geochemistry. Rev. Mineral. Geochem. 82, 219–287.
Teng, F.Z., Li, W.Y., Rudnick, R.L., Gardner, L.R., 2010. Contrasting lithium and magnesium isotope fractionation during continental weathering. Earth Planet. Sci. Lett. 300, 63–71.
Tipper, E.T., Galy, A., Gaillardet, J., Bickle, M.J., Elderfield, H., Carder, E.A., 2006. The magnesium isotope budget of the modern ocean: Constraints from riverine magnesium isotope ratios. Earth Planet. Sci. Lett. 250, 241–253.
Tipper, E.T., Gaillardet, J., Louvat, P., Capmas, F., White, A.F., 2010. Mg isotope constraints on soil pore-fluid chemistry: Evidence from Santa Cruz. California. Geochim. Cosmochim. Acta. 74, 3883–3896.
Tipper, E.T., Lemarchand, E., Hindshaw, R.S., Reynolds, B.C., Bourdon, B., 2012. Seasonal sensitivity of weathering processes: Hints from magnesium isotopes in a glacial stream. Chem. Geol. 312–313, 80–92.
Trostle, K.D., 2013. Magnesium isotope systematics in arid hawaiian soils.
Wang, S.J., Teng, F.Z., Rudnick, R.L., Li, S.G., 2015. The behavior of magnesium isotopes in low-grade metamorphosed mudrocks. Geochim. Cosmochim. Acta. 165, 435–448.
Wimpenny, J., Gíslason, S.R., James, R.H., Gannoun, A., Pogge Von Strandmann, P.A.E., Burton, K.W., 2010. The behaviour of Li and Mg isotopes during primary phase dissolution and secondary mineral formation in basalt. Geochim. Cosmochim. Acta. 74, 5259–5279.
Wimpenny, J., Colla, C.A., Yin, Q., Rustad, J.R., Casey, W.H., 2013. Investigating the Behaviour of Mg Isotopes during the Formation of Clay Minerals. Geochim. Cosmochim. Acta. 128, 178–194.
Wimpenny, J., Yin, Q.Z., Tollstrup, D., Xie, L.W., Sun, J., 2014. Using Mg isotope ratios to trace Cenozoic weathering changes: A case study from the Chinese Loess Plateau. Chem. Geol. 376, 31–43.
Young, E.D., Galy, A., 2004. The Isotope Geochemistry and Cosmochemistry of Magnesium. Rev. Mineral. Geochem. 55, 197–230.
Zamanian, K., Pustovoytov, K., Kuzyakov, Y., 2016. Pedogenic carbonates: Forms and formation processes. Earth-Sci. Rev. 157, 1–17.
Zhang, Z.J., Liu, C.Q., Zhao, Z.Q., Cui, L.F., Liu, W.J., Liu, T.Z., Liu, B.J., Fan, B.L., 2015. Behavior of redox-sensitive elements during weathering of granite in subtropical area using X-ray absorption fine structure spectroscopy. J Asian Earth Sci. 105, 418–429.
Zhang, Z.J., Mao, H.R., Zhao, Z.Q., Cui, L.F., Liu, C.Q., 2021. Sulfur dynamics in forest soil profiles developed on granite under contrasting climate conditions. Sci. Total Environ. 797, 149025.